COMPDYN 2013
4th ECCOMAS Thematic Conference on
Computational Methods in Structural Dynamics and Earthquake Engineering
M. Papadrakakis, V. Papadopoulos, V. Plevris (eds.)
Kos Island, Greece, 12–14 June 2013

SHEAR STRENGTH ASSESSMENT OF REINFORCED CONCRETE COLUMNS

Stamatina G. Chasioti[1], Konstantinos G. Megalooikonomou[2],

and Stavroula J. Pantazopoulou[2,3]

[1] IWB, University of Stuttgart
Pfaffenwaldring 4, 70569 Stuttgart, Germany
e-mail: stamatina.chasioti@iwb.uni-stuttgart.de

[2] Department of Civil and Environmental Engineering, University of Cyprus
P.O. Box 20537, 1687 Nicosia, Cyprus
kmegal01@ucy.ac.cy
pantazopoulou.stavroula@ucy.ac.cy

[3] on leave of absence from Democritus University of Thrace, Greece

Keywords: seismic assessment, shear strength, the modified compression field theory, inclination of the compression strut, columns, concrete web crushing.

Abstract. *Seismic assessment of reinforced concrete structures depends on strength values that can be estimated with sufficient accuracy only when the modes of failure are ductile. The level of accuracy degrades when considering brittle mechanisms of resistance, particularly when focusing on shear transfer and the associated deformation capacity. In this paper, it has been found that an important factor affecting the primary estimation of the shear strength is the inclination of the plane of sliding failure θ, identified as 45^o by the Mörsch truss, an assumption that does not comply with experimental results on columns. Using basic mechanics, the proposed model improves the correlation of the estimations, regarding both the concrete and transverse reinforcement contributions, V_c and V_s, presenting a new method for estimating θ, in particular in cases where applicability of the MCFT is limited by sparse stirrup spacing (i.e., assumptions about smearing of reinforcement are inappropriate). The concrete contribution component is established from first principles having as point of departure the fact that concrete directly supports shear only over the compression zone of the member, where cracks may be assumed to have closed. Conditions of concrete diagonal tension cracking and compressive crushing are both considered. Published experiments are used to guide and verify the development of the analytical model.*

1 INTRODUCTION

Explicit description of the load-deformation performance of structural elements is an essential ingredient of displacement-based seismic assessment procedures. Column elements are the most critical components for the safety of structure when the structure undergoes lateral sway as they carry the overbearing structure. The load-displacement curve is the envelope of the lateral shear – drift relationship; this follows the relationship of the characteristic Moment Rotation relationship of the element (since $V=M/L_s$), but apart from the basic flexural action, a number of premature phenomena may terminate the deformation capacity of the member. Syntzirma and Pantazopoulou (2010) used capacity based prioritizing of the modes of failure in order to identify the weakest mechanism of resistance so as to calculate the available deformation capacity of the member.

As a first step in seismic assessment of columns, flexural behavior is calculated from established procedures. The effect of shear is not taken into account in the approach but as an external acceptance criteria, in comparing the flexural force demand with the shear strength. The latter may be reduced for comparisons beyond flexural yielding, depending on displacement ductility (see EC8-III(2005), as an example). A great degree of uncertainty still dominates the shear strength response. Figure 1 compares the parametric sensitivity of the dominant equations for shear strength adopted by EC8-III (2005) and the ASCE/SEI 41 (2007) assessment guidelines for a simple case example. The greater source of discrepancy is the angle of the truss model that interprets the response of the member after diagonal web cracking. In the presence of densely detailed reinforcement the Modified Compression Field Theory (MCFT) could be used to calculate moment-shear-axial load interaction and to derive shear strength and response to deformation. However, an essential condition is smearing of reinforcement and stress and strain, which is not possible if reinforcement is sparse, as occurs in older construction. An alternative approach for lightly reinforced members, where the MCFT cannot be directly applied, has been pursued by Chasioti et al. (2012) whereby the plane of sliding failure after web cracking is associated with the principal tensile direction in the compression zone at the critical column cross section.

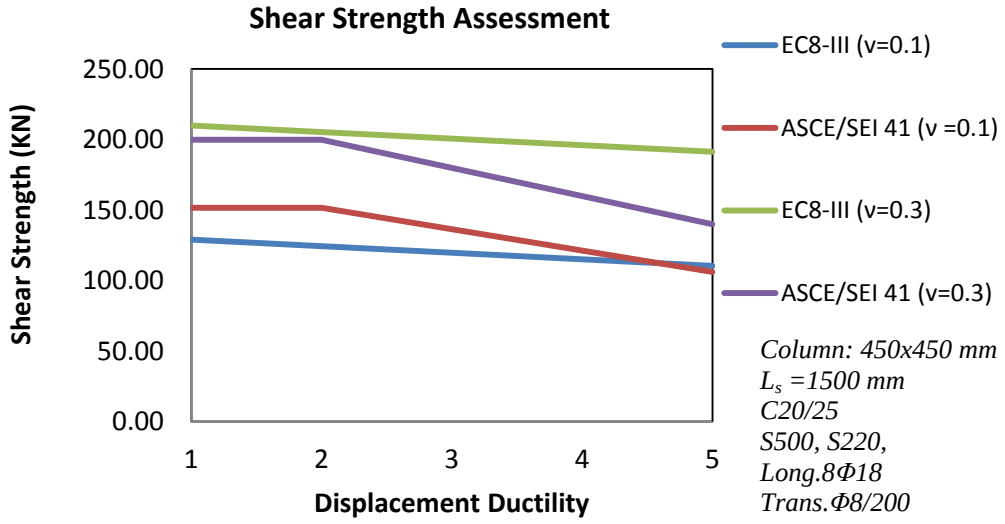

Figure 1: Shear Strength Assessment Example according to EC8-III and ASCE/SEI 41.

2 THE SHEAR TRANSFER MECHANISM

Traditionally, post cracking shear strength was estimated from summation of various separate contributions, attributed to concrete V_c (comprising shear transfer over the compression zone V_{cc}, and aggregate interlock and dowel action over the tension zone V_{ct}), to web reinforcement V_s and to axial load (Figure 2). It is a point of contention as to whether these mechanisms can actually be separated and independently estimated; it may be more honest to admit that these may be viewed as successive refinements to the underlying basic truss model that was inspired by Mörsch more than 100 years ago, so as to improve its correlation with the test data. Despite the departure of modern expressions from the original truss model, its origin should stay in focus: the concrete contribution was meant to be a correction over the truss term (web reinforcement) so as to match the test results. So the concrete contribution cannot be a significant portion of the strength (as it sometimes occurs in practical calculations when using the code expressions to severely undereinforced elements); this concern is only mentioned in the ASCE/SEI 41 (2007) where it is postulated that conforming elements are those where more than 75% of the available shear strength is owing to the web reinforcement term. Oddly enough, no particular attention is paid to the relative magnitude of the V_c and the V_s components of shear strength in EC8-III (2005).

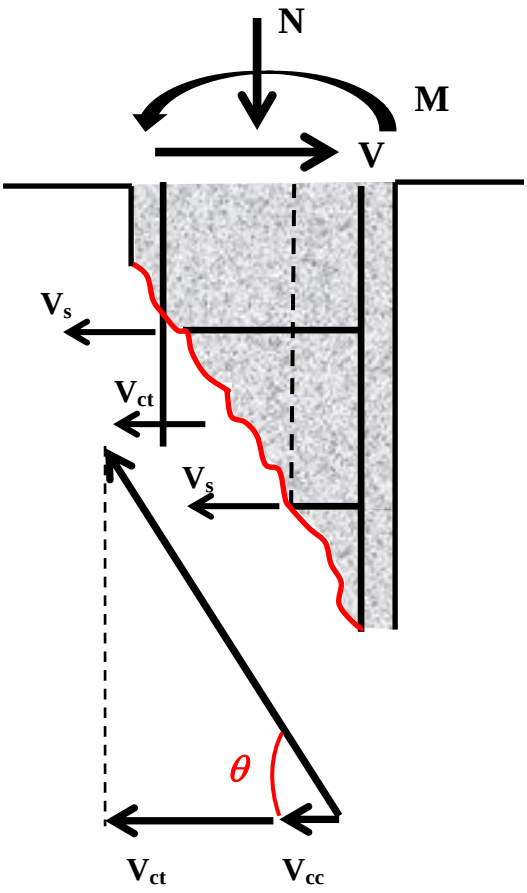

Figure 2: Free body diagram across a diagonal shear crack.

The presence of axial load in reinforced concrete columns (contrary to RC beams) is an important parameter which affects occurrence of diagonal cracking. This influence can be assessed both qualitatively and quantitatively. For example, compressive axial force delays di-

agonal tension cracking, increases the height of the compression zone of the member and increases the amount of shear force required to render the principal tensile stress of the web equal to the tensile strength of concrete.

Thus shear resistance to cracking increases with the axial load ratio whereas the value of the angle θ forming between the primary diagonal crack at tension failure, with the longitudinal axis of the member departs from the 45^o postulate. Actually, this particular variable has a critical influence on the determined strength since the inclination of the major sliding plane (i.e. the angle θ) determines the number of stirrup layers mobilized in shear, i.e., the V_s term in Eqn. 1. Several other variables appear to have a stronger influence, namely, the axial load magnitude, the aspect ratio of the member on shear strength and the effective area of the concrete section mobilized in the "concrete" shear contribution. In this paper these issues are explored from first principles and with particular reference to older type columns with non-ductile details under lateral sway.

$$V_n = V_c + V_s \tag{1}$$

3 THE STATE OF STRESS IN THE COMPRESSION ZONE

Both code procedures cited in the preceding refer to the effective web cross sectional area, ($0.8A_g$) in the estimation of concrete contribution to shear strength. It is believed that this assumption may be problematic, since open cracks prevent shear transfer under cyclic loads. To amend this counterintuitive argument, Syntzirma and Pantazopoulou (2006) introduced a requirement that the axial load ratio exceeds the difference between tension and compression reinforcement (ρ_{s1}-ρ_{s2}) as pre-requisite for consideration of the concrete contribution component. Recently, an alternative expression for the V_c term was considered, whereby it was postulated that only the part of the cross section that bears normal compression may be able to directly support shear stress in the presence of bending moment. So the effective area A_v, contributing to shear resistance is taken equal to $b_w \times c$. While is it generally acceptable that limited shear stress can also be developed in the tension zone of the cross section due to aggregate interlock , the statement above is on the safe side for the assessment phase. The depth of compression zone c and its location varies along the height of a column bent in double curvature and carrying a constant axial load N: consider the state of stress at the end cross-sections (terms with subscript e) as well as that at the column midheight (terms with subscript m) in Figure 3. Clearly, in the latter case, c_m extends over the entire depth of the cross section with the normal compressive stresses at the cross section being moderated as $\nu_o f_c$, where ν_o the axial load ratio in the column. To the contrary, in the end cross section normal stresses are localized within the depth of compression zone c_e, which supports a compressive force that is much higher than the net axial load, as illustrated in Fig. 3. Thus, the compressive stress resultant, F_{ce}, may be obtained from equilibrium as:

$$F_{ce}+\rho_{s2} b_w d f_{s2,e}-\rho_{s1} b d f_{s1,e}-N=0, \text{ thus, } F_{ce} = N+(\rho_{s1} f_{s1,e}-\rho_{s2} f_{s2,e}) b_w d \tag{2}$$

where the local compressive stress is,

$$\sigma_e=F_{ce}/b_w c_e, \text{ and } \nu_e=F_{ce}/b_w c f_c \quad i.e., \ \nu_e=\sigma_e/f_c \tag{3}$$

It is evident that the local stress intensity far exceeds the mean value, $\sigma_m = \nu_o f_c$ (where ν_o the normalized axial load ratio defined as, $\nu_o = N/(b_w d f_c)$) which occurs at the mid-height cross section.

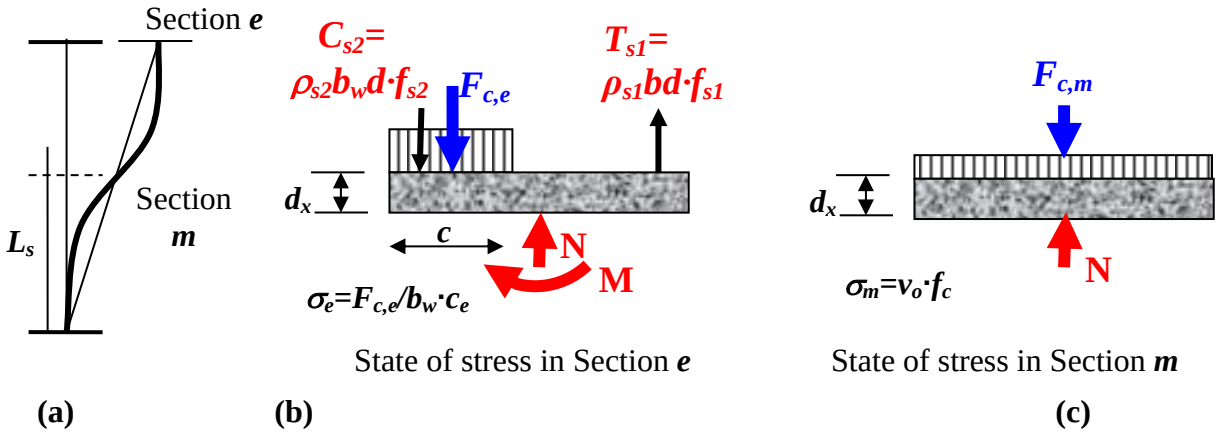

Figure 3: (a) Column under lateral sway, (b) Equilibrium of normal forces at section *e*, (c) Nominal normal forces at section *m*.

4 SHEAR FAILURE UNDER COMBINED LATERAL AND AXIAL LOAD

Members with non-ductile detailing are symptomatic of the older construction practices used in concrete structures up to only few years ago. In this context, a frequent example is the occurrence of high axial load ratios and large longitudinal reinforcement ratios. In these cases a brittle shear failure is often anticipated prior to the occurrence of flexural yielding. In order to evaluate the member's shear strength, the local state of stress depicted in Figure 3 need be considered as a point of reference for the calculation of the shear sliding plane. An assumption of this approach is that the sliding plane occurs along the main diagonal crack thereby defining the number of stirrups mobilized in tension and the geometry of the so-called variable angle truss model. Conditions of cracking considered refer to the state of stress in the compression zone where it is believed that the major concrete resistance to shear originates. In this direction, principal stress directions are considered for two possible events, namely: (a) diagonal tension failure in the compression zone, orthogonal to the compressive strut, (b) diagonal strut crushing failure due to excessive compression; a third mode of failure, which determines the basic strength of the variable angle truss model is associated to yielding of transverse reinforcement (case c). In each one of the first two modes the occurrence of cracking, either due to tensile stress or due to tensile strain (Poisson's effects) respectively, determines the sliding failure prior to flexural yielding at different stress levels and therefore they would result in different truss geometry. In this paper these two cases are referred to as two extreme conditions under which cracking may occur in the compression zone.

CASE A: Strength at Diagonal Tension Failure

With reference to Figure 3, for the end cross section *e* subjected to shear stress τ and normal stresses $\nu'_e = \nu_e f_c$, and $\sigma_{yy}=0$, the direction of principal tension may be determined by setting the associated principal tensile stress value equal to the tensile strength of concrete

f_{ctk}=0.5$\sqrt{f_c}$ at the onset of diagonal cracking of the web. This is evaluated from the following equation (considering the least – i.e., tensile – principal stress):

$$\underline{\sigma} = \begin{bmatrix} \sigma & \tau \\ \tau & 0 \end{bmatrix} \Rightarrow \sigma_{1,2} = \frac{v'_e}{2} \pm \sqrt{\tau^2 + \left(\frac{v'_e}{2}\right)^2} \Rightarrow -f_{ctk} = \frac{v'_e}{2} - \sqrt{\tau^2 + \left(\frac{v'_e}{2}\right)^2} \Rightarrow$$

$$\Rightarrow \tau^2 + \left(\frac{v'_e}{2}\right)^2 = \left(f_{ctk} + \frac{v'_e}{2}\right)^2 \Rightarrow \tau = \sqrt{f_{ctk} \cdot (f_{ctk} + v'_e)} = f_{ctk} \cdot \sqrt{1 + \frac{v'_e}{f_{ctk}}} \qquad (4)$$

The shear stress τ is related to the flexural moment at the end cross section when considering that $V=M/L_s$ where L_s is the member's shear-span:

$$\tau = \frac{V}{b_w \cdot c} = \frac{M}{b_w \cdot c \cdot L_s} \qquad (5)$$

Upon substitution to Eqn. 4, Eqn. 6 is obtained for ν'_e.

$$\tau = \frac{M}{b_w \cdot c \cdot L_s} = f_{ctk}\sqrt{1 + \frac{v'_e}{f_{ctk}}} \Rightarrow v'_e = \left[\left(\frac{M}{c \cdot b_w \cdot L_s \cdot f_{ctk}}\right)^2 - 1\right] \cdot f_{ctk} \qquad (6)$$

Parameter ν'_e represents the normal stress in the concrete compression zone of the member's end critical section for the case where cracking occurs due to diagonal tension i.e., when direct tension is transferred to the concrete compression zone via the lateral load (note that the value of the normalized longitudinal stress ν_e is much higher than $\nu_o = N/ f_c b_w d$ which represents the nominal axial load ratio reported in tests, a value that occurs at the point of inflection in the absence of flexural moment).

CASE B: Concrete Web Crushing (Axial Load Prevailing)

Consistently with Figure 3 and with the calculations above for the end cross section *e*, at the onset of concrete web crushing the principal compressive stress may be set equal to the compressive strength of concrete f_c. Solving accordingly the Eqn. 4 of the stress tensor for the plus sign (+) and substituting τ from the Eqn. 5, will result in ν''_e (Eqn. 7), which represents the normal stress at the end cross section at which concrete web crushing may occur. In this case, the combination of lateral load and high axial load is taken in consideration, with the axial load to be controlling failure and the inclination of the principal compression to be influenced by flexural and shear-stress combination. The result is a steeply inclined shear crack.

$$v''_e = \left[1 - \left(\frac{M}{c \cdot b_w \cdot L_s \cdot f_{ctk}}\right)^2\right] \cdot f_c \qquad (7)$$

Equations 6 and 7, estimate the normal stress in the cross section which will result in shear cracking owing to direct tension induced by the lateral load (case A), ν'_e, and owing to the concrete web crushing (case B), ν''_e. Both values depend on the values of the flexural moment *M*. Cases A and B both represent two extreme modes of failure, associating the flexural moment *M* in terms of forces acting to the member (stress resultant), to the cross section's normal stresses in the compression zone, ν'_e, and ν''_e respectively.

To facilitate immediate solution to this problem, values ν'_e, and ν''_e (from Eq. 6 and 7) are plotted against the compressive stress $\sigma_e=F_{ce}/b_w c_e$ (Eqn. 3) as a function of the bending moment *M*. Thus, the point of intersection of the resistance curve M- σ_e, to the either two potential failure curves will result in a critical combination of acting shear $V=M/L_s$, which determines the point of the shear crack initiation. Juxtaposition of the curves covers the com-

plete range of the member's response, starting with the uncracked cross section response in phase I all the way to flexural failure (here associated with 20% postpeak loss of the maximum carrying load).

CASE C: Cracking Due To Indirect Tension Induced From Compression Load

If the resistance curve M- σ_e does not intersect any of the two potential failure curves of the two failure modes referred to as cases A and B above, a check for cracking is performed in terms of strain. This is in recognition of the fact that diagonal tension failure may also occur indirectly due to lateral expansion in consideration of the Poisson's phenomenon. In such a situation, the point of shear crack initiation corresponds to a value of the moment M with a certain combination of τ and σ_e, where the longitudinal strain ε_{long} in the fiber where the concrete resultant F_c is applied, derives from a value of lateral strain ε_{lat} which is equal to the concrete tensile strain capacity. This is calculated from the ratio of concrete's tensile strength f_{ctk} divided by the concrete's modulus of elasticity E_c (Eqn. 8). Here, F_c is considered to be applied at the centroid of the compression zone, i.e. $0.4 \cdot c$ from the extreme compression fiber, where c the compression zone depth (on grounds of the established practice to represent the concrete stresses with a rectangular stress block extending over 80% of the depth of compression zone).

$$v \cdot \varepsilon_{long} = \varepsilon_{lat} = f_{ctk}/E_c \tag{8}$$

In Eq. (8), v is the Poisson's ratio, taken here equal to -0.25. For normal concrete strength class C20/25, $f_{ctk}=0.5\sqrt{f_c}$, and E_c=25000 MPa, the ε_{lat} is estimated as -0.00010 to -0.00015. Therefore, the point of shear crack in the resistance curve corresponds to a moment M in the end cross section with a longitudinal strain in the critical fiber in the direction of principal tension of $\varepsilon_{long,}$= (0.0001/0.25 = 0.0004) to (0.00015/0.25 = 0.0006).

The controlling case, A or B or C will define the point of initiation of shear cracking in the resistance curve with a specific combination of flexural moment $M_{cr,support}$, shear stress τ and normal stress σ_e. For a linear moment diagram (constant shear) along the shear span of the column, the flexural moment at distance d from the support, is equal to: $M_d=(L_s-d)\cdot M_{cr,support} / L_s$ when the moment at the face of the support equals $M_{cr,support}$. With reference to Eqn. 3 for the moment M_d the compression stress acting on the compression block is σ_d, while the shear stress τ remains approximately constant (assuming that the depth of compression zone is nearly the same as at the face of the support). The orientation of principal axes, ϑ, at the centroid of the compression zone a distance d from the support is obtained with reference to the longitudinal member axis, using basic mechanics according with Eqn. 9:

$$\tan 2\vartheta = \frac{2\tau}{\sigma_x - \sigma_y} = \frac{2\tau}{\sigma_d} \tag{9}$$

The number of the stirrups intersected by the shear plane is:

$$\frac{d-c}{s \cdot \tan\vartheta} \tag{10}$$

whereas the corresponding steel contribution, V_s, is obtained from the sum of forces of the total number of stirrup legs parallel to the plane of action and intersected by the inclined crack plane:

$$V_s = A_{s,tr} \cdot f_{y,tr} \cdot \frac{d-c}{s \cdot \tan\vartheta} \tag{11}$$

In Eq. (11), $A_{s,tr}$ is the total area of stirrups layers parallel to the plane of action, $f_{y,tr}$ the yield strength of the transverse steel, d the effective depth of the cross section, c the compression zone depth and s, the stirrup spacing.

The concrete contribution, is given by the shear stress resultant τ over the compression zone area of the critical section, $V_c = \tau \cdot 0.8 b_w \cdot c$

5 EXPERMENTAL CORROBORATION

Test specimens used in this paper in order to derive and calibrate the shear model were selected from among the available experimental literature with particular interest to the case of lightly reinforced members under constant axial load and cyclic displacement reversals simulating earthquake effects, where shear failure occurred prior to or immediately after flexural yielding. These are listed in Table 1. The cross section stirrup patterns are presented in Fig. 4; note that all the specimens considered had 90^0 hooks for anchorage of transverse reinforcement.

Tests No.1 to 4, failed in shear prior to flexural yielding and their experimental values regarding the shear strength serve as reference for comparison with the derived analytical values, since no degradation phenomena took place. Note that significant axial stresses are imposed on these columns, $P/f_c'A_g \approx 0.2\text{-}0.6$, which are raised substantially with increasing moment magnitude due to bending. In order to widen the range of possible axial load/implied moment combinations and to concentrate on the significance of the magnitude of the axial load on the column's shear performance, one more column was added to the database. Specimen No. 5 with a normalized axial load of 0.07 fails in shear immediately after the attainment of yielding.

Specimen ID; Serial No		**Mode of failure**	**angle** θ	**Geometry**				$P/f_c'A_g$	f_c' MPa	**Long. Reinf.**		**Transverse Reinf.**		
				b mm	h mm	L_s/d	a			D_{bl} mm	f_{yl} MPa	d_t mm	f_{yh} MPa	s mm
Spec. 1 [1]	1	S	28	457	457	3.75	1	0.32	33.0	8Ø28.7	445	9.5	372	457
Spec. 2 [1]	2	S	14	457	457	3.75	1	0.21	33.0	8Ø28.7	445	9.5	372	457
Spec. 3 [1]	3	S	13	457	457	3.75	1	0.62	17.0	8Ø32.3	445	9.5	372	457
X−9 [2]	4	S	18	267	267	1.60	2	0.50	28.6	12Ø12+4Ø16	395	6.0	270	100
2CLH18 [3]	5	FS	NA	457	457	3.83	1	0.07	33.1	8Ø25.4	331	9.5	400	457

[1]Woods and Matamoros (2010);[2] Lam et al (2003); [3]Lynn at al (1996); mode of failure, S: shear prior to flexural yielding, FS: shear after yielding ; angleθ: test value of the inclination of the sliding plane with respect to the longitudinal member's axis; b, h: cross section width and height, respectively; L_s/d: aspect ratio; P: axial load as % of $f_c'A_g$; f_c': concrete strength; D_{bl},f_{yl}: diameter and yield stress of longitudinal Reinf.; d_t,f_{yh}: diameter and yield stress of stirrups; s: spacing of stirrups.

Table 1: Test specimen materials and details (a is a cross section index with reference to Fig. 4)

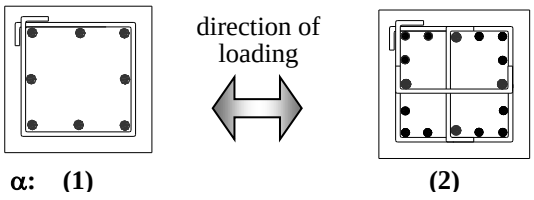

Figure 4: Cross section patterns of the specimens considered – in accordance with Table 1.

The theory presented in Chapter 4 was applied in the above specimens. For the specimens No 1 to 4 (Figures 6 to 9), the stress resultants were plotted versus only the moment values till

the point of flexural yielding (since these specimens failed prior to flexural yielding) whereas for the specimen No. 5 moment values were plotted for the entire range till the point of flexural failure while corresponds to the moment value M_u. The analysis for each specimen includes three diagrams. In the first one the values of normal stresses mentioned in Chapter 4 are plotted versus the moment M. In the second diagram, the blue curve corresponds to the lateral strain induced by the longitudinal of the third diagram as shown in Eqn. 8, while the red dashed line is the limiting value for the concrete's ultimate strain in tension. The curve of the third diagram shows the longitudinal strain of the fiber where the concrete resultant F_c is applied in the compression zone center of gravity in a distance of $0.4 \cdot c$ from the extreme compression fiber.

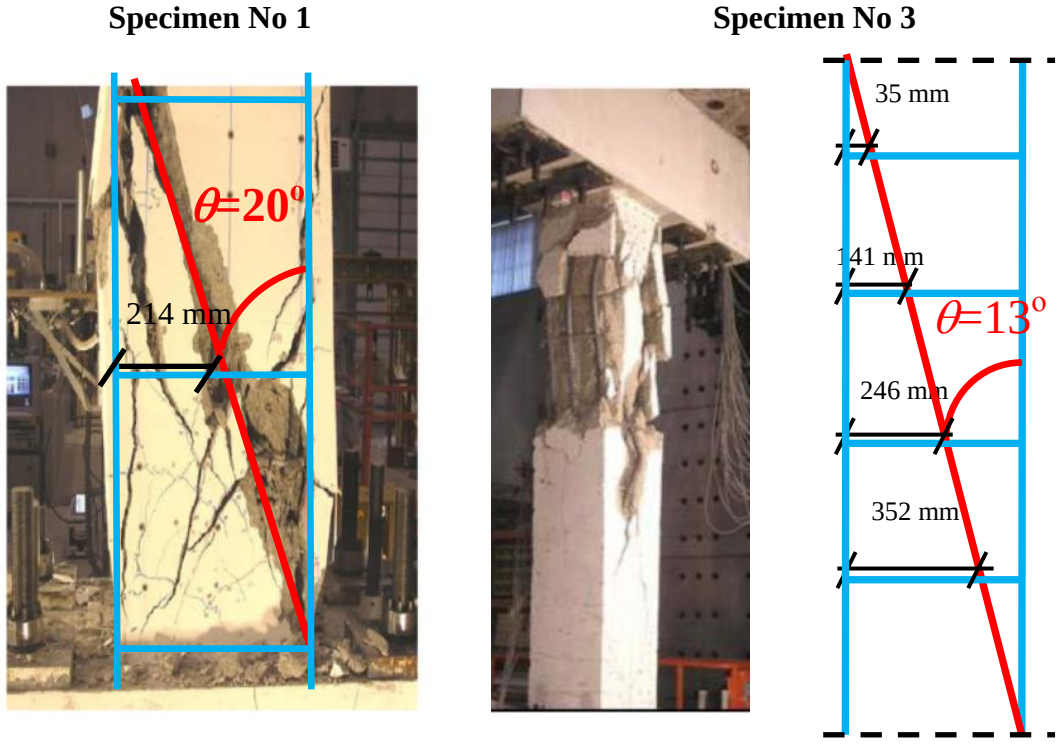

Figure 5: Truss geometry for the specimens 1 and 3.

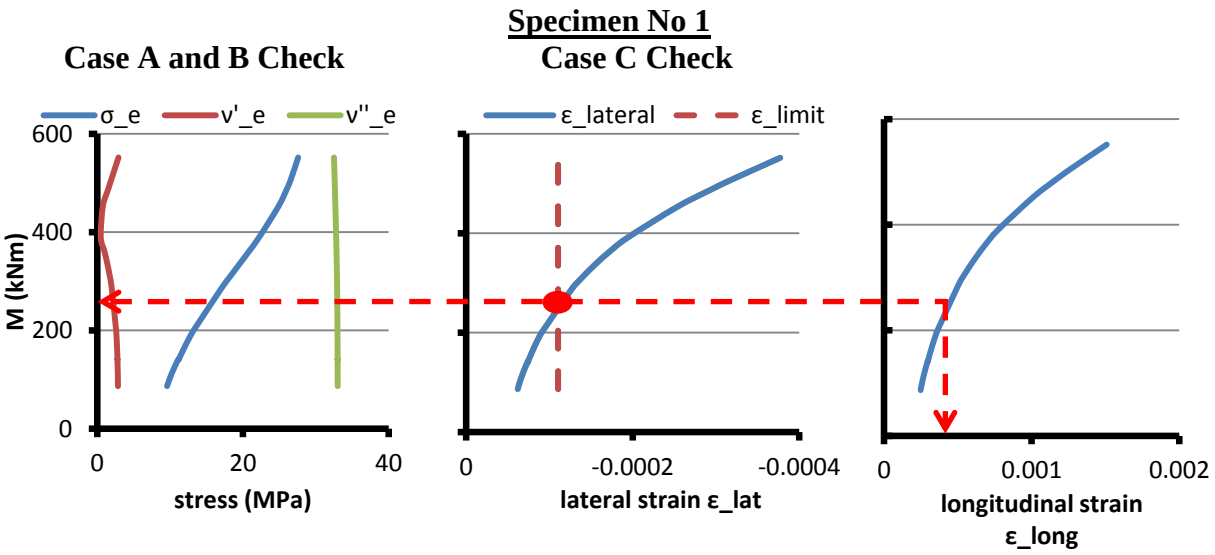

Figure 6: Analysis for the specimen No.1.

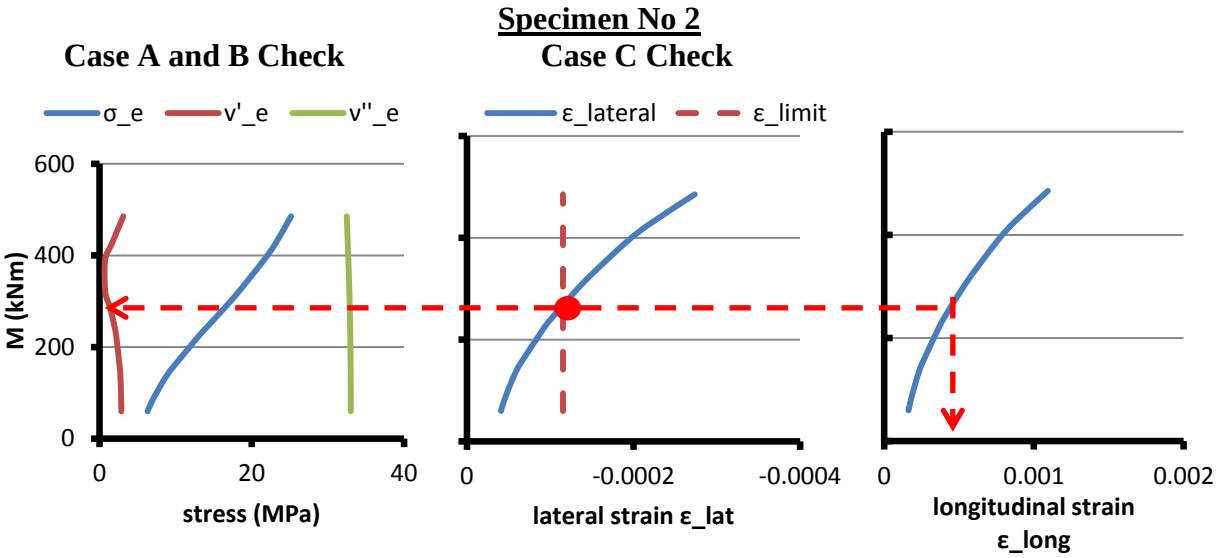

Figure 7: Analysis for the specimen No.2

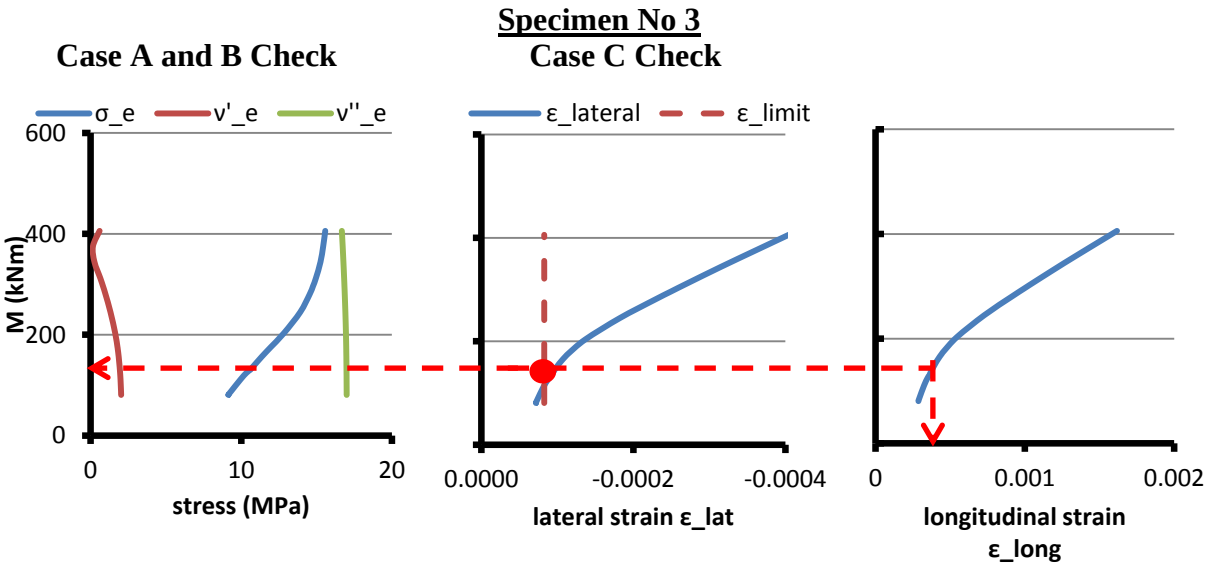

Figure 8: Analysis for the specimen No.3

Note that for the first four columns the point of the shear crack initiation comes from Case C as described in Chapter 4, i.e. lateral strain of the compression zone fiber where the concrete resultant is applied exceeds the concrete's ultimate tensile strain. Excessive axial load in all first four columns induces increased compression stresses in the compression block and delays cracking avoiding the case of diagonal tension failure. Specimen No. 5 has similar geometry and material properties to specimen No.1 as shown in Table 1, with the only difference the low axial load. Shear crack initiation is controlled in this case from Check A, i.e. diagonal tension failure is the prevailing mode, and the point of intersection of the blue and red curve precedes the point of cracking from criterion C as depicted by the second diagram of Figure 10.

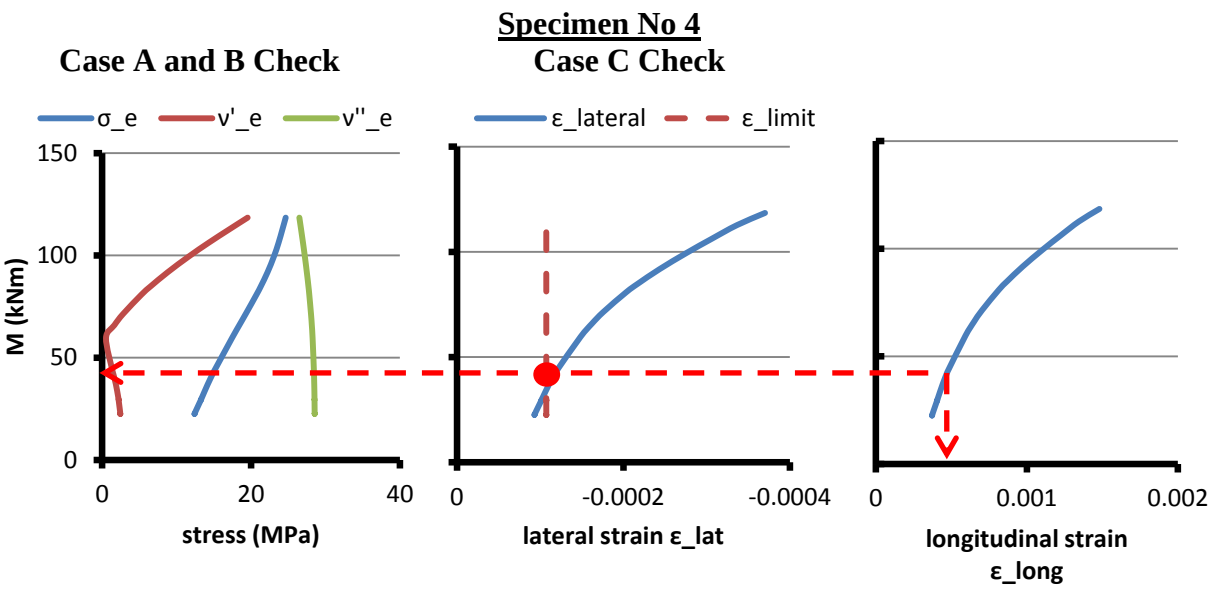

Figure 9: Analysis for the specimen No.4.

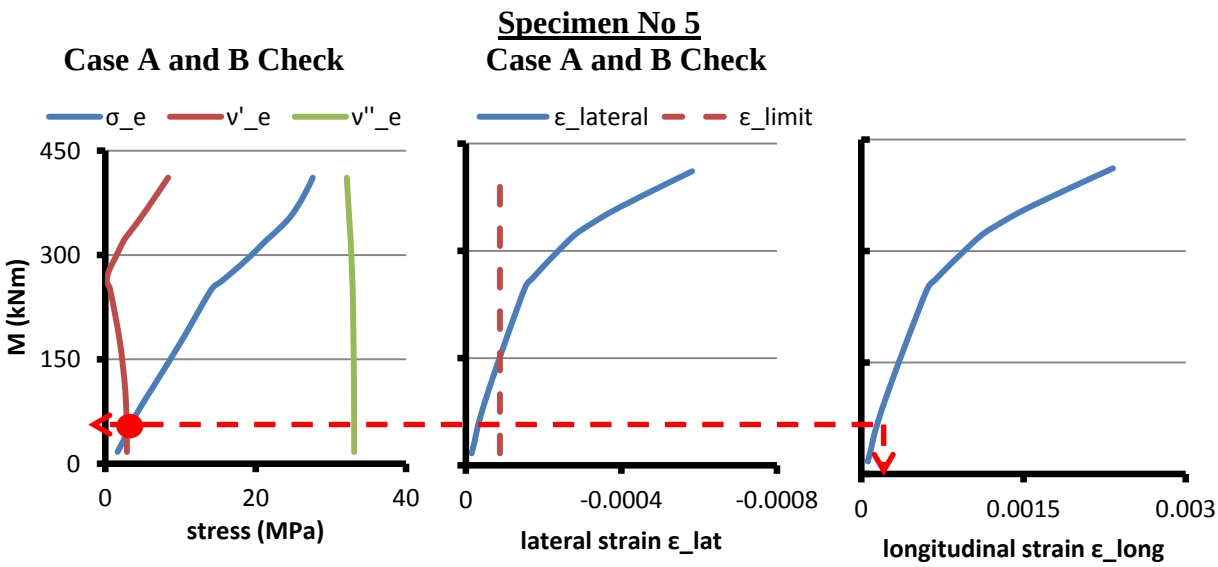

Figure 10: Analysis for the specimen No.5.

After assessment of the states of stress and strain as described above, the moment values which correspond to face of the support at shear failure for specimens No 1 to 5 are: 288, 276, 124, 37 and 52 kNm, whereas the corresponding values at d from the support are, 211, 202, 91, 14 and 38 respectively. The inclination of the angle θ is estimated for the second set of moment values for all five columns, as follows: 9^o, 10^o, 3^o, 8^o and 5^o respectively. Figure 11 shows the correlation between the shear strength values as obtained from the test data versus the estimated values according to the proposed model. Furthermore, the proposed procedure seems consistent with the basic inception of concrete contribution as a minor correction to the estimations of the truss model for shear strength (i.e. that the concrete contribution V_c is ought to be a significantly smaller component than V_s, Figure 12).

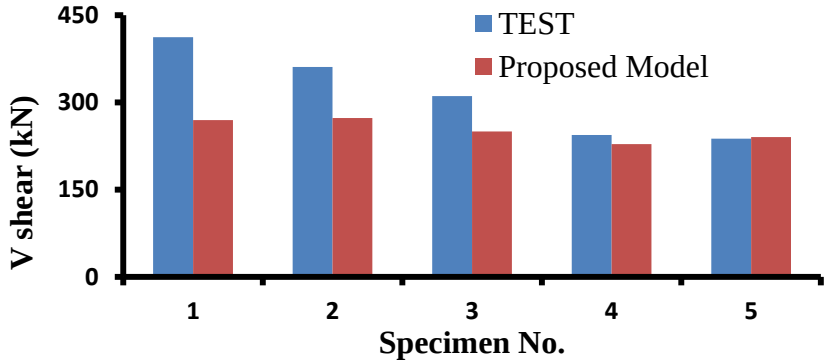

Figure 11: Shear strength test values vs. predicted values as calculated according to the proposed model.

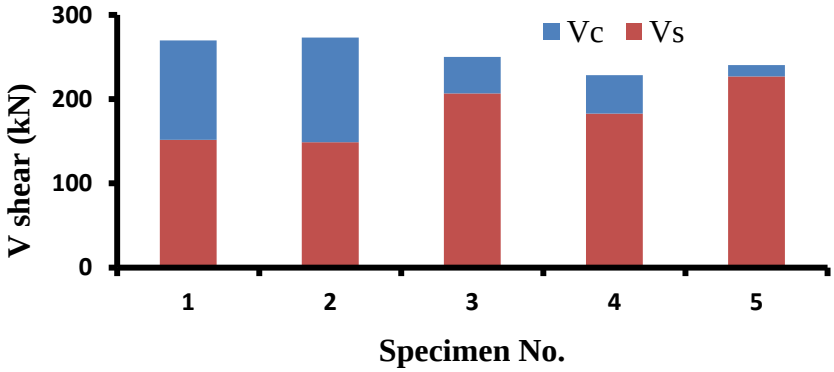

Figure 12: Concrete *Vc* and steel *Vs* contribution indices proportional to the total shear strength estimate.

6 CONCLUSIONS

This paper presents results of an analytical investigation aiming to establish shear strength in lightly reinforced columns where shear failure is driven by sparsely spaced stirrups. In such situations the assumptions of the MCFT theory about smearing of reinforcement are not appropriate, and the state of stress is primarily established with reference to the concrete cross section. To quantify the participation of web reinforcement and concrete to shear strength at the occurrence of the primary plane of failure, it is postulated that this is defined by diagonal tension cracking in the compression zone of the member owing to the combined action of shear stresses and axial stresses in that part of the cross section. Diagonal tension cracking is determined either from exceedance of tensile stress (due to combined shear action) or tensile lateral (expansion) strain due to Poisson's effects. This enables definition not only of the effective shear stress that may be carried in the compression zone but also the flexural moment associated with the onset of shear failure, as well as the number of stirrups intersected by the sliding plane (and therefore contributing to shear resistance). The methodology is tested against the available tests in the literature which are marked by shear failure in sparsely reinforced columns with either high or low axial load, in all cases producing good correlation with reported modes of failure and attained lateral load strength.

REFERENCES

[1] B. Martin-Perez, S. J. Pantazopoulou, Mechanics of Concrete Participation in Cyclic Shear Resistance of RC. *Journal of Structural Engineering*, ASCE, **124 (6)**, 633-641, 1998.

[2] M.J.N. Priestley, R. Verma, Y. Xiao, Seismic Shear Strength of Reinforced Concrete Columns. *Journal of Structural Engineering*, ASCE, **120 (8)**, 2310-2329, 1994.

[3] Tureyen, A.K. and Frosch, R.J. (2003). Concrete shear strength: Another perspective. *ACI Structural Journal **10:5***,609-615.

[4] Lam, S.S.E., Wu, B., Wong, Y.L., Wang, Z.Y., Liu, Z.Q. and Li, C.S. (2003), Drift capacity of rectangular reinforced concrete columns with low lateral confinement and high-axial load. *ASCE Journal of Structural Engineering **129:6***,733-742.

[5] Sezen, H. and Moehle, J. (2004). Strength and deformation capacity of R.C. columns with limited ductility. *13thWorld Conference on Earthquake Engineering*. No 279.

[6] Woods, C. and Matamoros, A.B. (2010). Effect of longitudinal reinforcement ratio on the failure mechanism of R/C columns most vulnerable to collapse. *9thU.S. National and 10th Canadian Conference on Earthquake Engineering*. No 1636.

[7] ASCE/SEI 41 (2007). Seismic Rehabilitation of Existing Buildings, American Society of Civil Engineers.

[8] CEB-FIP Model Code (2010). Chapter 6:Interface Characteristics; Chapter 7:Design.

[9] Elwood, K., Matamoros, A., Wallace, J., Lehman, D., Heintz, J., Mitchell, A., Moore, M., Valley, M., Lowes, L., Comartin, C., and Moehle, J. (2007), Update to ASCE/SEI 41 Concrete Provisions. *Earthquake Spectra* **23:3**,493-523.

[10] Eurocode 8 (2005). Design of structures for earthquake resistance – Part.3: Assessment and retrofitting of buildings, European Committee for Standardisation.

[11] FEMA 356 (2000). Prestandard and commentary for the seismic rehabilitation of buildings, Federal Emergency Management Agency.

[12] Pantazopoulou, V. and Syntzirma, D. (2009). Code expressions for deformation capacity of lightly reinforced concrete members – a comparative study. *ACES Workshop: Advances in Performance-Based earthquake Engineering.*

[13] Syntzirma, D.V., and Pantazopoulou, S.J. (2006), Deformation capacity of R.C. members with brittle details under cyclic loads. ACI Special Publication **Vol. 236:** 1-22.

[14] ACI 318-99 (1999), Building Code Requirements for Structural Concrete, American Concrete Institute.

[15] Syntzirma, D.V., and Pantazopoulou, S.J. (2010), Deformation capacity of lightly reinforced concrete members – comparative evaluation. *ACES Workshop: Advances in Performance-Based earthquake Engineering*, Series Geotechnical, Geological, and Earthquake Engineering, Vol. 13, Springer.

[16] Chasioti S.G., Pantazopoulou S.J. and Syntzirma D.V. (2012), "Seismic Assessment of Lightly Reinforced Buildings: A Study of Shear Demand VS. Supply", *15th World Conference on Earthquake Engineering*, Lisbon, Portugal, September 24-28, 2012.

[17] Lynn, A., Moehle, J.P., Mahin, S., and Holmes, W. (1996), Seismic evaluation of existing R.C. building columns. *Earthquake Spectra* ***12:4***, 715-739.